

Adiabatic evolution of a coupled-qubit Hamiltonian

V. Corato and P. Silvestrini

*Second University of Naples-INFN, Via Roma 29, I-81031 Aversa, Italy
and Istituto di Cibernetica del CNR, Via Campi Flegrei 34, I-80078 Pozzuoli, Italy*

L. Stodolsky

Max-Planck-Institut für Physik (Werner-Heisenberg-Institut), Föhringer Ring 6, 80805 München, Germany

J. Wosiek

M. Smoluchowski Institute of Physics, Jagellonian University, Reymonta 4, 30-059 Cracow, Poland

(Received 10 April 2003; revised manuscript received 23 June 2003; published 11 December 2003)

We present a general method for studying coupled qubits driven by adiabatically changing external parameters. Extended calculations are provided for a two-bit Hamiltonian whose eigenstates can be used as logical states for a quantum CNOT gate. From a numerical analysis of the stationary Schrödinger equation we find a set of parameters suitable for representing CNOT, while from a time-dependent study the conditions for adiabatic evolution are determined. Specializing to a concrete physical system involving superconducting quantum interference devices (SQUID's), we determine reasonable parameters for experimental purposes. The dissipation for SQUID's is discussed by fitting experimental data. The low dissipation obtained supports the idea that adiabatic operations could be performed on a time scale shorter than the decoherence time.

DOI: 10.1103/PhysRevB.68.224508

PACS number(s): 03.67.Lx, 74.50.+r, 85.25.Dq

I. INTRODUCTION

The basic elements for processing quantum information (e.g., to perform quantum computation¹) are quantum bits (qubits), namely, two-level systems exhibiting quantum coherence between the states, quantum register (arrays of qubits), and quantum gates.² Computations are performed by the creation of quantum superpositions of the qubits and by controlled entanglement of the information on the qubits.³ The main goal of any physical implementation of a quantum information-processing device is therefore to control systems of coupled qubit with a phase-coherence time long enough to permit the necessary manipulations. Various physical systems have been proposed for the physical implementation of qubits, including photons,⁴ trapped ions,⁵ spins in nuclear magnetic resonance (NMR),⁶ electrodynamic cavities,⁷ and semiconductor quantum dots,⁸ to mention some of the most popular. Other experiments and proposals focus on superconducting Josephson devices, where almost macroscopic (mesoscopic) devices such as Josephson junctions,⁹ superconducting quantum interference devices (SQUID's),¹⁰ or Cooper pair boxes,¹¹ that is, devices fabricated in condensed-matter physics, are brought to behave quantum mechanically. These devices promise certain advantages such as large-scale integration and fabrication as well as ease of integration with conventional electronics. To manipulate qubits quantum gates are necessary, that is, logic devices capable of operating on linear combinations of input states.

Among the possible mechanisms for manipulating coupled qubits, adiabatic procedures¹² are of special interest. Quantum adiabatic evolution provides a natural framework for solving combinatorial search problems on quantum computers.¹³ Any problem which can be recast as the minimization of an energy function (which can then be converted

into a quantum Hamiltonian) can potentially be solved by adiabatic quantum computation. General problems have been treated numerically, and studies of a set of exact cover instances designed to be hard have shown polynomial behavior out to instances containing as many as 20 bits.¹⁴ Whereas a conventional quantum algorithm is implemented as a sequence of discrete unitary transformations that form a quantum circuit involving many energy levels of the computer, the adiabatic algorithm works by keeping the state of the quantum computer close to the instantaneous ground state of a Hamiltonian that varies continuously in time. Therefore, an imperfect quantum computer implementing a conventional quantum algorithm might experience different sorts of errors than an imperfect adiabatic quantum computer. In fact, an adiabatic quantum computer has an inherent robustness against errors that might enhance the usefulness of the adiabatic approach.¹⁵ Local operations on single qubits (such as NOT¹⁶) or two coupled qubits (such as the adiabatically controlled CNOT gate we shall discuss^{17,18}) are also possible, where adiabatic operations take place as a sequence of discrete transformations acting on a few qubits at a time. In this line it is important to study a possible tradeoff between the advantages of error reduction due to adiabatic evolution and the longer times required for gate operations.

In this paper we will explain some general principles for studying adiabatic SQUID qubit operations focusing particularly on a CNOT gate, and present numerical calculations relevant to the behavior and design of such systems.

II. COUPLED-QUBIT HAMILTONIAN

In discussing coherence properties of the SQUID under adiabatic inversion, we have suggested its interest for the

elements of the ‘‘quantum computer.’’¹⁶ The single-bit NOT operation can be realized by adiabatic inversion. The next most complicated operation is the two-bit operation CNOT, with which a computer may, in principle, be constructed. CNOT is a two-qubit operation and we will try to represent it by two interacting double-potential well systems. Qualitatively, we will use the procedure of performing an adiabatic NOT on the first qubit while trying to influence its behavior by the state of the second. We will find a region of parameter space where this works.

In the one-dimensional or one SQUID problem one has a Schrödinger equation in the variable Φ with a kinetic term and the potential term,

$$U = \frac{(\Phi - \Phi^{ext})^2}{2L} - \frac{I^c \Phi_0}{2\pi} \cos(2\pi\Phi/\Phi_0), \quad (1)$$

which for small Φ yields a double-well potential. I^c and L are the Josephson critical current and the inductance of the superconducting ring, respectively, while Φ^{ext} is an applied external flux. When Φ^{ext} is swept slowly as a function of time, as explained in Ref. 16, an adiabatic inversion or level crossing can be induced, amounting to a realization of the NOT operation. If the state is originally in the left potential well it is transferred to the right well and vice versa, implying a reversal of the current direction in the superconducting ring.

We now wish to investigate this idea of quantum gates generated by adiabatic transformations to systems of more than one variable, in particular for the two variable CNOT operation. Although we are only concerned here with two SQUID's, we briefly indicate a method valid for many qubits. The equation for an array of underdamped flux-linked rf SQUID's is

$$\Phi - \Phi^{ext} = Li. \quad (2)$$

In this equation Φ and i are meant as column vectors representing all the fluxes Φ_j and currents i_j in the j th rf SQUID loop, Φ^{ext} is the column vector corresponding to the external fluxes, while L is a matrix representing the self and mutual inductances. The current i_j in j th ring is expressed in terms of the capacitance C_j and the superconducting Josephson current I_j :

$$i_j = -C_j \dot{\Phi}_j - \frac{1}{R} \Phi_j - I_j^c \sin \Phi_j \frac{2\pi}{\Phi_0}, \quad (3)$$

where $\Phi_0 = hc/2e = 2 \times 10^{-7}$ G cm² is the superconducting flux quantum and R is the effective resistance of the junction.

An important property of L , by the reciprocity of mutual inductances, is that L is a symmetric matrix. As we need i for the linear homogeneous system of Eq. (3), we invert L :

$$i = L^{-1}(\Phi - \Phi^{ext}). \quad (4)$$

Since L is symmetric, L^{-1} is also symmetric. Neglecting the dissipative term, we now have Eq. (3) as

$$-\sum_k L_{jk}^{-1}(\Phi - \Phi^{ext})_k - I_j^c \sin \Phi_j \frac{2\pi}{\Phi_0} = C_j \dot{\Phi}_j \quad (5)$$

that can be written as

$$-\frac{\partial U}{\partial \Phi_j} = C_j \dot{\Phi}_j \quad (6)$$

by introducing the potential

$$U = \frac{1}{2} \sum_{j,k} L_{jk}^{-1}(\Phi - \Phi^{ext})_k(\Phi - \Phi^{ext})_j - \left(\frac{\Phi_0}{2\pi}\right) \sum_j I_j^c \cos \Phi_j \frac{2\pi}{\Phi_0}. \quad (7)$$

Finally, switching to the reduced dimensionless flux variable $\phi = \Phi(2\pi/\Phi_0)$ the last two equations become

$$-\frac{\partial U}{\partial \phi_j} = \left(\frac{\Phi_0}{2\pi}\right)^2 C_j \dot{\phi}_j, \quad (8)$$

$$U = \left(\frac{\Phi_0}{2\pi}\right)^2 \frac{1}{2} \sum_{j,k} L_{jk}^{-1}(\phi - \phi^{ext})_k(\phi - \phi^{ext})_j - \left(\frac{\Phi_0}{2\pi}\right) \sum_j I_j^c \cos \phi_j. \quad (9)$$

To make this situation look more symmetric, we follow recent practice and introduce the shifts $\phi \rightarrow \phi + \pi$, $\phi^{ext} \rightarrow \phi^{ext} + \pi$, which move the maximum of the $\cos \phi$ term to $\phi = 0$.¹⁹ This does not affect the quadratic term, but it must be kept in mind that $\phi^{ext} = 0$ now corresponds to a nonzero applied field. We thus have finally

$$U \rightarrow U = \left(\frac{\Phi_0}{2\pi}\right)^2 \frac{1}{2} \sum_{j,k} L_{jk}^{-1}(\phi - \phi^{ext})_k(\phi - \phi^{ext})_j + \left(\frac{\Phi_0}{2\pi}\right) \sum_j I_j^c \cos \phi_j, \quad (10)$$

where henceforth we use the shifted variables.

A. Two variables

We now specialize to two SQUID's, called 1 and 2, with variables ϕ_1, ϕ_2 . In the absence of mutual inductance, each one can be thought of as a qubit, whose dynamics is described by a double-well potential. For CNOT we shall think of ϕ_1 as the target bit and ϕ_2 as the control bit. We shall apply a sweeping flux ϕ_1^{ext} and would like that this sweeping flux induce an adiabatic inversion if the control bit is $|1\rangle$ (e.g., current flowing clockwise in SQUID 2), and not induce this inversion if the control bit is $|0\rangle$ (current flowing in the opposite direction in SQUID 2).

For the two-variable system the matrix $L = \begin{pmatrix} L_{11} & L_{12} \\ L_{12} & L_{22} \end{pmatrix}$ can be inverted, giving

$$L^{-1} = \frac{1}{L_1 L_2 - L_{12}^2} \begin{pmatrix} L_2 & -L_{12} \\ -L_{12} & L_1 \end{pmatrix}. \quad (11)$$

L_{12} , the mutual inductance between the two rings, could be controlled experimentally by a further device with Josephson junctions²⁰ and switched off for convenience in performing other operations.

Writing out U we obtain

$$U = \left(\frac{\Phi_0}{2\pi}\right)^2 \frac{1}{2} \frac{1}{L_1 L_2 - L_{12}^2} [L_2(\phi_1 - \phi_1^{ext})^2 + L_1(\phi_2 - \phi_2^{ext})^2 - 2L_{12}(\phi_1 - \phi_1^{ext})(\phi_2 - \phi_2^{ext})] + \left(\frac{\Phi_0}{2\pi}\right) I_1^c \cos \phi_1 + \left(\frac{\Phi_0}{2\pi}\right) I_2^c \cos \phi_2. \quad (12)$$

Let us first look at this potential with the ϕ^{ext} zero, and imagine varying ϕ_1 at fixed ϕ_2 . For $L_{12}=0$, we would simply have the usual symmetric double-potential well for ϕ_1 . Now as L_{12} is turned on, a tilt is introduced into this ϕ_1 potential. A coupling term $\sim L_{12}\phi_1\phi_2$ is added providing a bias in the potential for ϕ_1 , so that the double well is asymmetric even though $\phi_1^{ext}=0$. The direction of this bias depends on whether ϕ_2 is positive or negative.

If we think of ϕ_2 as essentially fixed, and now suppose sweeping ϕ_1^{ext} , we see that this sweep will either increase the asymmetry present in the double well, or decrease it. If the wells are caused to be further separated, we have no inversion, if the wells are brought together and cross, we will have an inversion and a ‘‘NOT.’’ Which case occurs will depend on the sign of ϕ_2 . The condition for CNOT is accomplished: according to the state of ϕ_2 , an inversion takes place or does not take place in the ϕ_1 variable.

The discussion is more convenient if we introduce dimensionless parameters

$$\frac{1}{L} = \sqrt{\frac{L_1 L_2}{L_1 L_2 - L_{12}^2}}, \quad \beta_1 = \frac{2\pi}{\Phi_0} L I_1^c, \quad \beta_2 = \frac{2\pi}{\Phi_0} L I_2^c, \quad (13)$$

as well as the dimensionless inductances

$$l_1 = \frac{L_1}{\sqrt{L_1 L_2}}, \quad l_2 = \frac{L_2}{\sqrt{L_1 L_2}}, \quad l_{12} = \frac{L_{12}}{\sqrt{L_1 L_2}}. \quad (14)$$

We may then write Eq. (12) as

$$U = \left(\frac{\Phi_0}{2\pi}\right)^2 \frac{1}{L} \left\{ \frac{1}{2} [l_1(\phi_1 - \phi_1^{ext})^2 + l_2(\phi_2 - \phi_2^{ext})^2 - 2l_{12}(\phi_2 - \phi_2^{ext})(\phi_1 - \phi_1^{ext})] + \beta_1 \cos \phi_1 + \beta_2 \cos \phi_2 \right\}. \quad (15)$$

With this potential the Schrödinger equation for the wave function $\psi(\phi_1, \phi_2, t)$ is

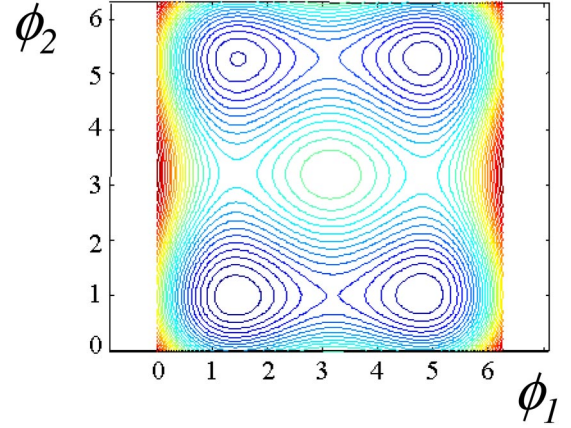


FIG. 1. (Color online) Potential as in Eq (22), with its four wells. The coordinate ϕ_1 (target bit) runs horizontally and ϕ_2 (control bit) vertically.

$$i\dot{\psi} = \mathcal{H}\psi \quad (16)$$

with Hamiltonian

$$\mathcal{H} = \frac{-1}{2C_1 \left(\frac{\Phi_0}{2\pi}\right)^2} \frac{\partial^2}{\partial \phi_1^2} + \frac{-1}{2C_2 \left(\frac{\Phi_0}{2\pi}\right)^2} \frac{\partial^2}{\partial \phi_2^2} + U. \quad (17)$$

Introducing

$$C = \sqrt{C_1 C_2} \quad (18)$$

as the typical capacitance, and defining the energy scale

$$E_0 = 1/\sqrt{LC} \quad (19)$$

\mathcal{H} can be cast in the form of an energy times a dimensionless Hamiltonian

$$\mathcal{H} = E_0 H, \quad (20)$$

$$H = \frac{-1}{2\mu_1} \frac{\partial^2}{\partial \phi_1^2} + \frac{-1}{2\mu_2} \frac{\partial^2}{\partial \phi_2^2} + V \quad (21)$$

with

$$V = V_0 \left\{ \frac{1}{2} [l_1(\phi_1 - \phi_1^{ext})^2 + l_2(\phi_2 - \phi_2^{ext})^2 - 2l_{12}(\phi_2 - \phi_2^{ext})(\phi_1 - \phi_1^{ext})] + \beta_1 \cos \phi_1 + \beta_2 \cos \phi_2 \right\}, \quad (22)$$

and the dimensionless parameters

$$\mu_1 = C_1 E_0 \left(\frac{\Phi_0}{2\pi}\right)^2, \quad \mu_2 = C_2 E_0 \left(\frac{\Phi_0}{2\pi}\right)^2, \quad V_0 = \sqrt{C/L} \left(\frac{\Phi_0}{2\pi}\right)^2. \quad (23)$$

Figure 1 shows the equipotential contours of $V(\phi_1, \phi_2)$, with its four potential wells.

We use natural units: $\hbar = 1$, $c = 1$, $e^2/\hbar c = 1/137$, thus $\Phi_0 = hc/2e = \pi\sqrt{137}$, and $(\Phi_0/2\pi)^2 = 137/4 = 34.3$; also $\sqrt{\text{farad/henry}} = 30$. Using these values

$$\begin{aligned}\mu_1 &\approx 1030 \sqrt{\left(\frac{C_1}{C_2}\right)^{1/2} \frac{C_1/\text{pF}}{L/\text{pH}}}, \\ \mu_2 &\approx 1030 \sqrt{\left(\frac{C_2}{C_1}\right)^{1/2} \frac{C_2/\text{pF}}{L/\text{pH}}}, \quad V_0 \approx 1030 \sqrt{C/\text{pF}}\end{aligned}\quad (24)$$

Note that these parameters are not all independent, as the following relation exists:

$$\sqrt{\mu_1\mu_2} = V_0. \quad (25)$$

That is, the three basic dimensional quantities C_1 , C_2 , and L have been exchanged for two dimensionless parameters and the overall energy scale E_0 .

III. CNOT BY ADIABATIC INVERSION

With SQUID qubits, the logical states are the flux states of the superconducting rings (with one qubit $|0\rangle$ or $|1\rangle$, with two qubits $|0\rangle|1\rangle$, $|1\rangle|1\rangle$, and so forth), whereas the Hamiltonian eigenstates are in general a linear combination of them. In case of two coupled qubits to form CNOT, each logical state of the gate will be represented by a wave function localized in one of the four distinct minima of the potential of Eq. (22). The four states can be labeled as 1,2,3,4 and placed in a tableau of the kind $\begin{pmatrix} 4 & 3 \\ 1 & 2 \end{pmatrix}$, where the locations refer to Fig. 1. That is, in the tableau the positions of the numbers indicate in which well of Fig 1 the state is localized while the numbers themselves indicate which energy eigenstate is meant. The lowest-energy eigenstate is “1,” and the highest of the four first states “4.”

A CNOT operation is defined by the following conditions: (A) the control bit does not change its state and (B) the target bit is reversed or not reversed, according to whether the control bit is $|1\rangle$ or $|0\rangle$. In the tableau representation, a physical embodiment of CNOT would be

$$\begin{pmatrix} 4 & 3 \\ 1 & 2 \end{pmatrix} \rightarrow \begin{pmatrix} 4 & 3 \\ 2 & 1 \end{pmatrix}. \quad (26)$$

Condition (A) on the stability of the control bit is exhibited in that no states move between the top and bottom row. Condition B) is realized in that the top row remains unchanged while the bottom row is “flipped.”

Realization of operations such as Eq. (26) can be accomplished by using adiabatic processes, thanks to the “no level crossing” behavior of adiabatic evolution. The no-crossing property assures that a state initially in the first, or second, or third, . . . energy level will end up in the first, or second, or third, . . . energy level after the adiabatic evolution, while at the same time the logical state associated with the level may be changing.

One can proceed as follows. We first search for an initial Hamiltonian whose variable external parameters $(\phi_1^{ext}, \phi_2^{ext})$

are adjusted to give the first four energy eigenstates localized in the four different minima of Fig. 1. Then, we search for a final Hamiltonian where another set of $(\phi_1^{ext}, \phi_2^{ext})$ gives the tableau on the right of Eq. (26). In this procedure we need only to study the *stationary* Schrödinger equation at first. After having determined some suitable parameter sets, we shall also study the full time-dependent Schrödinger equation to determine what sweep speed is “slow” in order to guarantee adiabatic behavior.

For the present paper we defer a detailed discussion of the phases the states acquire during the time evolution. These phases contain dynamic and geometric contributions²¹ and they themselves can be used for quantum information processes.²² For a given set of parameters and sweep conditions the phases can of course be calculated explicitly and in no way affect the general applicability of the results and procedures presented here. Calculations of phases will be reported upon in future work.

We obtain²³ the switching behavior according to Eq. (26) by fixing the control bias ϕ_2^{ext} at a relatively high value, while an adiabatic sweep of the target bias ϕ_1^{ext} occurs. This is a generalization of a NOT (Ref. 16) on ϕ_1 . The presence of the l_{12} coupling produces an extra bias on the target bit which “helps or hinders” the NOT operation. The relatively large bias on ϕ_2 comes from condition (A): we attempt to “immobilize” the control bit despite the perturbations communicated by the sweep of ϕ_1^{ext} via l_{12} . We therefore investigate the region $|\phi_1^{ext}| \ll |\phi_2^{ext}|$. If ϕ_2 is indeed successfully immobilized, it will be fixed in one of its two potential wells and can have only the values $\phi_2 \approx \pm 1$. As seen by ϕ_1 , these two states amount to an extra bias which is added or subtracted to ϕ_1^{ext} . To linear order (since we take all $\phi_1^{ext}, \phi_2^{ext}$ small compared to 1 and ϕ_1, ϕ_2 are in the neighborhood of 1) and introducing the notation $\phi_{1\text{eff}}^{ext} = \phi_1^{ext} \pm l_{12}/l_1$ the potential terms involving ϕ_1 in Eq. (22) become

$$\begin{aligned}-2l_1\phi_1\phi_1^{ext} - 2l_{12}\phi_1(\pm 1) &= -2l_1\phi_1\left(\phi_1^{ext} \pm \frac{l_{12}}{l_1}\right) \\ &= -2l_1\phi_1\phi_{1\text{eff}}^{ext},\end{aligned}\quad (27)$$

so that there is an effective shift in the external bias on ϕ_1 by $(\pm l_{12}/l_1)$. According to Eq. (27) the bias condition for switching from one tableau to another is given by $|\phi_1^{ext}| = l_{12}/l_1$.

By a numerical study where we find essentially exact solutions of the Schrödinger equation for our potential, we find that there is indeed a region of $\phi_1^{ext}, \phi_2^{ext}$ plane where the eigenstates of Eq. (21) are well defined and behave as in this description. These regions are shown in the gray areas of Figs. 2(a) and 2(b). By well defined we mean that the expectation values of ϕ_1, ϕ_2 are at the location of one of the wells $\approx (\pm 1, \pm 1)$, that only one of the first four levels is so localized, and finally that the dispersion of each coordinate $\sqrt{\langle \phi^2 \rangle - \langle \phi \rangle^2}$ is small compared to the expectation value of ϕ , which itself is in the neighborhood of 1. For the cases we present here, the ratio of the dispersion to the expectation value was in the vicinity of 0.3.

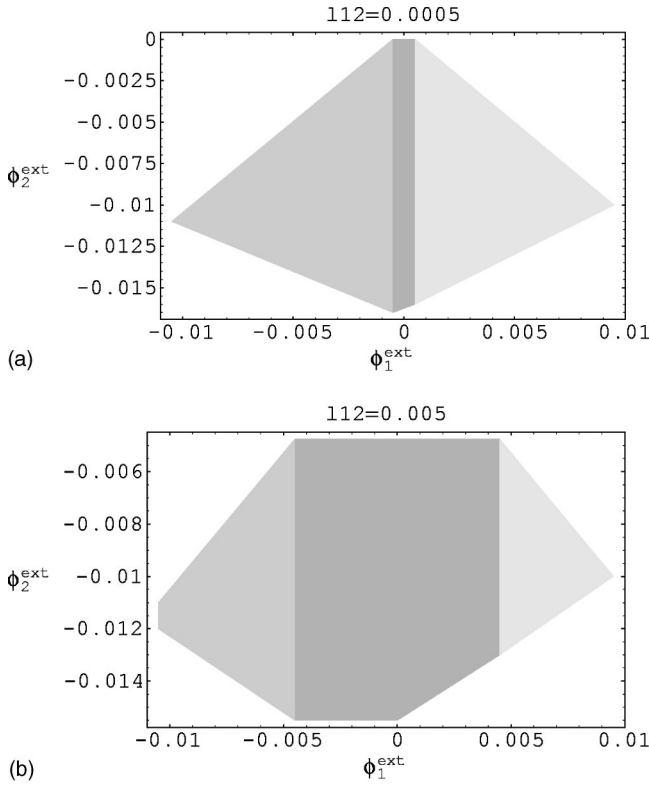


FIG. 2. (a) A region of the $\phi_1^{ext}, \phi_2^{ext}$ plane with a well-defined set of wave functions as explained in the text. The coupling parameter is $l_{12}=0.0005$. The other parameters are $l_1=l_2=1$, $\beta_1=\beta_2=1.19$, $\mu_1=\mu_2=V_0=16.3$. (b) As in (a) with coupling parameter $l_{12}=0.005$.

We find that the three different gray areas of Fig. 2(a) and 2(b) have well-defined tableaux as follows:

$$\begin{pmatrix} 3 & 4 \\ 1 & 2 \end{pmatrix}, \begin{pmatrix} 4 & 3 \\ 1 & 2 \end{pmatrix}, \begin{pmatrix} 4 & 3 \\ 2 & 1 \end{pmatrix}, \quad (28)$$

for the intermediate gray region (left), the darkest region (center), and the light gray region (right), respectively. On the order of 10–20 points were used to determine the boundaries in the figures. These tableaux fit with the description arrived at in the “immobilization” model, where either the top or bottom row inverts as we go from the central region to large $|\phi_1^{ext}|$. Hence a sweep from the central region to the right region will produce the desired mapping of Eq. (26). Similarly sweeping from the right region to the center and from the left region to the central region and vice versa can also serve as realizations, differing simply in the assignment of (0,1) for the bits or the names (1,2) for the SQUID’s. Note that the switch between tableaux occurs quite close to $|\phi_1^{ext}|=|l_{12}/l_1|$, as predicted by Eq. (27).

Concerning the time-dependent problem, the important time scale in the present context is τ_{adiab} , the shortest time in which an operation can be performed adiabatically. This time is relevant with respect to decoherence and relaxation effects, since the operation must take place in a time short compared to decoherence and relaxation times. An estimate for τ_{adiab} for the NOT operation¹⁶ gives

$$\tau_{adiab} = \epsilon \omega_{tunnel}^{-2} = \epsilon \tau_{osc}^2, \quad (29)$$

where ϵ is the asymmetry of the potential and $\omega_{tunnel}^{-1} = \tau_{osc}$ the inverse tunneling energy or oscillation time between the two states. Since here we also perform a kind of NOT, we expect a similar relation to hold, where ω_{tunnel} or τ_{osc}^{-1} is the smallest level splitting during the adiabatic passage and ϵ may be read off as the energy shift of the wells at the beginning and end of our sweep. A set of reasonable SQUID parameters for CNOT are $L_1=300$ pH, $L_2=280$ pH, $L_{12}=1.8$ pH, $C_1=C_2=0.1$ pF, and $I_1^c=I_2^c=1.45$ μ A. Since in frequency units $E_0 \approx [1/\sqrt{L/\text{pH } C/\text{pF } 1000}]$ GHz these values give $E_0 \approx 185$ GHz and $\tau_{adiab} \approx 2.7 \times 10^{-9}$ s. Preliminary results are in agreement with this estimate,¹⁸ and the question will be studied in more detail in further numerical work.

IV. IMPLEMENTATION

A. Dissipation

As with all discussions of quantum computation, the important open questions concern dissipative effects. These include the decoherence time τ_{dec} , or its inverse the decoherence rate D , as well as relaxation processes, represented by a time τ_{relax} .

These will affect adiabatic processes as we can see by examining the inversion or NOT process for a single qubit. With an increasing loss of phase coherence as caused by D , we expect the situation to become more and more “classical” and finally, when D is very large, the inversion is inhibited.¹⁶ Furthermore, after the inversion is completed there will be some tendency of the upper-energy state to relax to the lower-energy state.

We illustrate these effects in Fig. 3 where we show the probability for an inversion as a function of sweep time τ_{sweep} . Note that the times involved are much longer than the above estimate for the adiabatic time of 2.7×10^{-9} s, so the adiabatic condition should be satisfied. Starting at the left, we see that the probability of inversion is one until τ_{sweep} approaches τ_{dec} . For τ_{sweep} much longer than τ_{dec} it falls to 0.5, the “decohered” limit. For longer times, as τ_{sweep} approaches and passes τ_{relax} , the final result depends on which state we started with. Evidently in this limit we will always end up in the ground state, so the inversion probability is one if we started with the ground state (solid line) and zero if we started in the excited state (dotted line).

The times used were $\tau_{dec}=0.2$ μ s and $\tau_{relax}=0.2$ ms. The early part of the curve was found using the plots in Fig. 5 of the second part of Ref. 16 with this value of τ_{dec} , while the relaxation effects were found from the calculations shown in Fig. 7 of this reference. The value τ_{dec} used was based on the estimate $D=T/R e^2$,¹⁶ with $R=1$ M Ω at $T=40$ mK.

It is evident, as exemplified by the latter formula, that a necessary and—less evident—perhaps also a sufficient condition for quantum behavior of the system is a low classical dissipation. In the present context this implies a large value

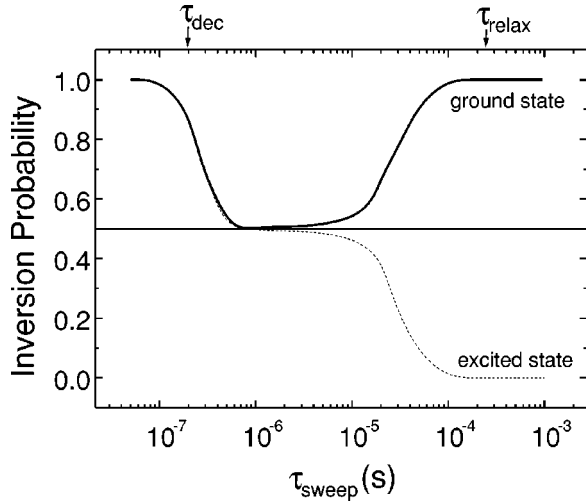


FIG. 3. The probability of inversion as a function of sweep time. The inversion probability is one until the sweep time approaches τ_{dec} , then it falls to about 0.5. When τ_{sweep} is increased toward τ_{relax} and greater, the system always ends in the lowest state, so the inversion probability is one if the initial state is the ground state, while it falls to zero for starting in the excited state. SQUID parameters used for the simulation were $\beta_L=1.2$, the loop inductance $L=400$ pH, the junction capacitance $C=0.1$ pF, the effective resistance $R=1$ M Ω , and the temperature $T=40$ mK

of R . Therefore we present some experimental data on this point, collected in the thermal regime for superconducting devices based on SQUID's.²⁴

In order to evaluate the dissipation of our system, we measured the transitions between adjacent flux states of the rf SQUID as a function of the external flux ϕ^{ext} . In the absence of noise, the escape from the metastable well would occur at a critical value of the external flux ϕ^c . Thermal noise induces transitions at random values of ϕ^{ext} smaller than ϕ^c , whose probability distribution, namely, $P(\phi^{ext})$ was measured by standard "time fly technique," as explained in the third reference listed in Ref. 9.

By fitting the data for P versus ϕ^{ext} with Kramers theory²⁵ in the extremely low-damping limit, with L , I_c , and C independently measured, we can obtain the effective resistance R . We introduce a dimensionless parameter $Q \sim R$, defined as $Q = \omega_0 RC$, where ω_0 is the small oscillation frequency. With decreasing temperature Q is large, showing a small dissipation at low temperatures. The plot of Fig. 4 indicates an exponential increase of R , and using the measured parameters we obtain $R=22$ k Ω at $T=2.9$ K. This is encouraging if the $D=T/Re^2$ estimate is correct, where we needed 1 M Ω at $T=40$ mK. The exponential fit shows that the effective resistance R is determined by tunneling of thermally activated quasiparticles, as expected when the external noise has been filtered out and only the intrinsic dissipation acts.

B. System design

On-chip integrated dc SQUID's can be used to read out the flux states,¹⁰ while the manipulation of the superconduct-

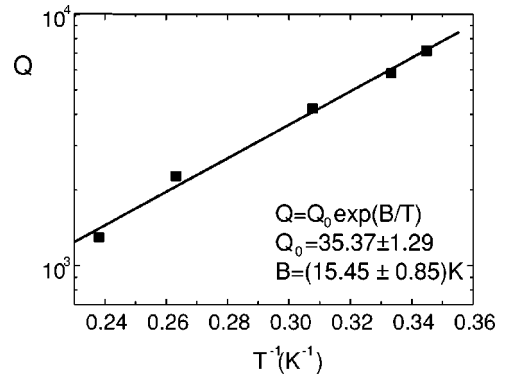


FIG. 4. Q factor as a function of the inverse of the temperature obtained by switching flux measurements (Ref. 24). Q increases exponentially with decreasing temperature, following the exponential law $Q=Q_0 \exp(B/T)$, with $Q_0=35.37$ and $B=15.45$ K. This behavior shows a strongly decreasing dissipation with temperature, and that the dissipation mechanism is essentially due to the tunneling of thermally activated quasiparticles in the Josephson junction.

ing qubits can be controlled by on-chip superconducting electronics. The coupling between the probe and the readout system could be through a superconducting transformer. While the intrinsic dissipation can be considerably reduced at low temperatures as explained above,^{9,10} a major cause of difficulty can be the spurious interaction of the qubit with readout and control devices.

In a good design, the readout device could be turned off during the manipulation. The technology to control this coupling may need to be developed, but could be reasonably provided by stacked junctions,²⁰ or small double-junction loop,¹⁹ interrupting the coupling transformers. The coupling is then controlled by external current signals. A further possibility is the development of a fast switch using simple single-flux quantum circuitry for switching the interaction on and off.²⁶

In conclusion we have presented a general method for studying the adiabatic evolution of a Hamiltonian describing a multiqubit system, controlled by varying external parameters. Detailed calculations were provided for a two-qubit Hamiltonian, whose eigenstates can be used as logical states for a quantum CNOT gate. From the numerical analysis of the stationary Schrödinger equation we obtained sets of parameters suitable to perform a CNOT operation, and indicated how a time-dependent study determines the limits for adiabatic evolution. Specializing to a definite physical system involving SQUID's, we identified reasonable values of the parameters, estimated effects due to dissipation, and considered some points of system design.

ACKNOWLEDGMENTS

The authors are grateful to C. Granata and B. Ruggiero for useful discussions and comments on experimental perspectives. This work was partially supported by MIUR-FIRB under project "Nanocircuiti Superconduttivi."

- ¹D.P. DiVincenzo, *Science* **270**, 255 (1995); C.H. Bennet and D.P. DiVincenzo, *Nature (London)* **404**, 247 (2000).
- ²A. Barenco, C.H. Bennett, R. Cleve, D.P. DiVincenzo, N. Margolus, P. Shor, T. Sleator, J.A. Smolin, and H. Weinfurter, *Phys. Rev. A* **52**, 3457 (1995).
- ³For a general overview on the argument see, for instance, *Macroscopic Quantum Coherence and Quantum Computing*, edited by D. Averin, B. Ruggiero, and P. Silvestrini (Kluwer Academic Plenum, Dordrecht, New York 2001).
- ⁴J.W. Pan, C. Simon, C. Brukner, and A. Zeilinger, *Nature (London)* **410**, 1067 (2001); E. Lombardi, F. Sciarrino, S. Popescu, and F. de Martini, *Phys. Rev. Lett.* **88**, 070402 (2002).
- ⁵J.I. Cirac and P. Zoller, *Phys. Rev. Lett.* **74**, 4091 (1995); C. Monroe, D.M. Meekhof, B.E. King, W.M. Itano, and D.J. Wineland, *ibid.* **75**, 4714 (1995); C.A. Sackett, D. Kielpinski, B.E. King, C. Langer, V. Meyer, C.J. Myatt, M. Rowe, Q.A. Turchette, W.M. Itano, D.J. Wineland, and C. Monroe, *Nature (London)* **404**, 256 (2000).
- ⁶N.A. Gershenfeld and I.L. Chuang, *Science* **275**, 350 (1997); M. Nielsen, E. Knill, and R. Laflamme, *Nature (London)* **396**, 52 (1998); J.A. Jones, M. Mosca, and R.H. Hansen, *ibid.* **393**, 344 (1998).
- ⁷Q.A. Turchette, C.J. Hood, W. Lange, H. Mabuchi, and H.J. Kimble, *Phys. Rev. Lett.* **75**, 4710 (1995); M. Brune, F. Schmidt-Kaler, A. Maali, J. Dreyer, E. Hagley, J.M. Raimond, and S. Haroche, *ibid.* **76**, 1800 (1996); A. Rauschenbeutel, G. Nogues, S. Osnaghi, P. Bertet, M. Brune, J.M. Raimond, and S. Haroche, *Science* **288**, 2024 (2000).
- ⁸D. Loss and D.P. DiVincenzo, *Phys. Rev. A* **57**, 120 (1998); T.H. Oosterkamp, T. Fujisawa, W.G. van der Wiel, K. Ishibashi, R.V. Hijman, S. Tarucha, and L.P. Kouwenhoven, *Nature (London)* **395**, 873 (1998); G. Burkard, D. Loss, and D.P. DiVincenzo, *Phys. Rev. B* **59**, 2070 (1999).
- ⁹Y. Yu, S. Han, X. Chu, S. I. Chu, and Z. Wang, *Science* **296**, 889 (2002); J.M. Martinis, S. Nam, J. Aumentado, and C. Urbina, *Phys. Rev. Lett.* **89**, 117901 (2002); P. Silvestrini, V.G. Palmieri, B. Ruggiero, and M. Russo, *ibid.* **79**, 3046 (1997).
- ¹⁰I. Chiorescu, Y. Nakamura, C.J.P.M. Harmans, and J.E. Mooij, *Science* **299**, 1869 (2003); J. Friedman, V. Patel, W. Chen, S.K. Tolpygo, and J.E. Lukens, *Nature (London)* **406**, 43 (2000); C. Granata, V. Corato, L. Longobardi, M. Russo, B. Ruggiero, and P. Silvestrini, *Appl. Phys. Lett.* **80**, 2952 (2002).
- ¹¹Yu.A. Pashkin, T. Yamamoto, O. Astafiev, Y. Nakamura, D.V. Averin, and J.S. Tsai, *Nature (London)* **421**, 823 (2003); Y. Nakamura, Yu.A. Pashkin, and J.S. Tsai, *ibid.* **398**, 786 (1999); D. Vion, A. Aassime, A. Cottet, P. Joyez, H. Pothier, C. Urbina, D. Esteve, and M.H. Devoret, *Science* **296**, 886 (2002); Y. Makhlin, G. Schon, and A. Shnirman, *Nature (London)* **398**, 305 (1999); J.P. Pekola, J.J. Toppari, M. Aunola, M.T. Savolainen, and D.V. Averin, *Phys. Rev. B* **60**, R9931 (1999).
- ¹²A. Messiah, *Quantum Mechanics North-Holland (Amsterdam, 1961)*.
- ¹³E. Farhi, J. Goldstone, S. Gutmann, and M. Sipser, quant-ph/0001106; T. Kadowaki and H. Nishimori, *Phys. Rev. E* **58**, 5355 (1998).
- ¹⁴E. Farhi, J. Goldstone, S. Gutmann, J. Lapan, A. Lundgren, and D. Preda, *Science* **292**, 472 (2001).
- ¹⁵M. Childs, E. Farhi, and J. Preskill, *Phys. Rev. A* **65**, 012322 (2002).
- ¹⁶P. Silvestrini and L. Stodolsky, *Phys. Lett. A* **280**, 17 (2001); in *Macroscopic Quantum Coherence and Quantum Computing*, edited by D. Averin, B. Ruggiero, and P. Silvestrini (Kluwer Academic Plenum, New York, 2001), p. 271; cond-mat/0004472 (unpublished).
- ¹⁷D.V. Averin, *Solid State Commun.* **105**, 659 (1998); D.V. Averin, *Nature (London)* **398**, 748 (1999).
- ¹⁸V. Corato, P. Silvestrini, L. Stodolsky, and J. Wosiek, *Phys. Lett. A* **309**, 206 (2003).
- ¹⁹R. Rouse, S. Han, and J.E. Lukens, *Phys. Rev. Lett.* **75**, 1614 (1995).
- ²⁰C. Granata, V. Corato, A. Monaco, B. Ruggiero, M. Russo, and P. Silvestrini, *Appl. Phys. Lett.* **79**, 1145 (2001).
- ²¹M.V. Berry, *Proc. R. Soc. London, Ser. A* **392**, 45 (1984).
- ²²J.A. Jones, V. Vedral, A. Ekert, and G. Castagnoli, *Nature (London)* **403**, 869 (2000); G. Falci, R. Fazio, G.M. Palma, J. Siewert, and V. Vedral, *ibid.* **407**, 355 (2000).
- ²³Our numerical methods are described in J. Wosiek, *Nucl. Phys. B* **644**, 85 (2002); J. Wosiek, hep-th/0204243 (unpublished).
- ²⁴B. Ruggiero, V. Corato, C. Granata, L. Longobardi, S. Rombetto, and P. Silvestrini, *Phys. Rev. B* **67**, 132504 (2003).
- ²⁵A. Kramers, *Physica (Amsterdam)* **7**, 284 (1940); M. Buttiker, E.P. Harris, and R. Landauer, *Phys. Rev. B* **28**, 1268 (1983).
- ²⁶R. C. Rey-de-Castro, M.F. Bocko, A.M. Herr, C.A. Mancini, and M.J. Feldman, *IEEE Trans. Appl. Supercond.* **11**, 1014 (2001).